

Newcastle disease virus-induced caspase-independent apoptosis pathway in BHK-21 cells

Chen-Wei Wang

Department of Veterinary Medicine, College of Veterinary Medicine, National Pingtung University of Science and Technology

Chia-Ying Lin

Da Dian Biotechnology Company Limited

Sheng-Chang Chung

Department of Veterinary Medicine, College of Veterinary Medicine, National Pingtung University of Science and Technology

Wen-Ling Shih

Department of Biological Science and Technology, National Pingtung University of Science and Technology

Tzu-Chieh Lin

International Degree Program in Animal Vaccine Technology, National Pingtung University of Science and Technology

Duangsuda Thongchan

Faculty of Agriculture and Technology, Rajamangala University of Technology Isan, Surin campus

hung-yi wu (✉ wuhy@g4e.npust.edu.tw)

National Pingtung University of Science and Technology Department of Veterinary Medicine Department of Veterinary Medicine <https://orcid.org/0000-0001-5748-8105>

Research

Keywords: Newcastle disease virus, Apoptosis, Caspase-independent pathway

Posted Date: May 11th, 2021

DOI: <https://doi.org/10.21203/rs.3.rs-449586/v1>

License:  This work is licensed under a Creative Commons Attribution 4.0 International License.

[Read Full License](#)

1 Newcastle disease virus-induced caspase-independent apoptosis pathway
2 in BHK-21 cells

3

4 Chen-Wei Wang¹, Chia-Ying Lin², Sheng-Chang Chung¹, Wen-Ling
5 Shih³, Tzu-Chieh Lin⁴, Duangsuda Thongchan⁵, Hung-Yi Wu^{1*}

6 1. Department of Veterinary Medicine, College of Veterinary

7 Medicine, National Pingtung University of Science and Technology,

8 No.1, Shuefu Rd., Neipu, Pingtung 91201, Taiwan.

9 2. Da Dian Biotechnology Company Limited, No. 21, Aly. 22, Ln. 77,

10 Hengnan Rd., Hengchun Township, Pingtung County 946001,

11 Taiwan

12 3. Department of Biological Science and Technology, National

13 Pingtung University of Science and Technology, No.1, Shuefu Rd.,

14 Neipu, Pingtung 91201, Taiwan.

15 4. International Degree Program in Animal Vaccine Technology,

16 National Pingtung University of Science and Technology, No.1,

17 Shuefu Rd., Neipu, Pingtung 91201, Taiwan.

18 5. Faculty of Agriculture and Technology, Rajamangala University of
19 Technology Isan, Surin campus, 145 Moo 15 Surin-Prasat Road,
20 Nokmuang, Muang District, Surin Province, Thailand, 32000

21

22 *Correspondence author: Hung-Yi Wu (DVM, PhD); Department of
23 Veterinary Medicine, College of Veterinary Medicine, National Pingtung
24 University of Science and Technology, 1 Shuefu Road, Neipu, Pingtung
25 91201, Taiwan; wuhy@g4e.npust.edu.tw

26

27 **Abstract**

28 **Background:** Newcastle disease virus (NDV) is an important virus for
29 humans. It is highly lethal in fowl and is newly identified as an oncolytic
30 virus for cancer treatment. *In vivo*, NDV induces spleen, thymus, bursa,
31 and mesenteric gland cell apoptosis, thereby causing immunosuppression.
32 *In vitro*, NDV can induce apoptosis by caspase-dependent pathways
33 including the mitochondria-mediated pathway and death
34 receptor-mediated pathway.

35 **Methods:** In this study, the major materials were baby hamster kidney
36 (BHK-21) cells, NDV virus (*Miyadera* strain; $10^{3.8}$ TCID₅₀/μl), and
37 pan-caspase inhibitor Z-Val-Ala-DL-Asp-fluoromethylketone
38 (z-VAD-fmk). All of the experiments used a viral infection MOI of 1.
39 Apoptosis was confirmed using DNA fragmentation and TUNEL assay.
40 Finally, the apoptosis-independent pathway was confirmed by western
41 blot analysis and immunofluorescence.

42 **Results:** In this study, we differentiate between the caspase group and
43 caspase inhibition group (added 100 μM pan-caspase inhibitor
44 [z-VAD-fmk]) in BHK-21 cells treated with NDV at 0, 12, and 24 h. In

45 the DNA fragmentation and TUNEL assays, the apoptosis appears at 12 h
46 and apoptosis increases over time, regardless of caspase or not. In protein
47 level determination, the antiapoptotic protein Bcl-2 decreased over time,
48 which is the opposite of how the proapoptotic proteins Bax, cytochrome
49 C, Mst3, and AIF behaved. Further, using western blot and
50 immunofluorescent staining, we checked the AIF and Endo G
51 translocation from the mitochondria (cytoplasmic) to the nucleus. In
52 addition to apoptosis, we found that NDV treatment of BHK-21 cells
53 decreased actin, regardless of caspase. The actin always decreased in the
54 NDV-treated BHK-21 cells at 12 and 24 h.

55 **Conclusions:** NDV-mediated BHK-21 cell apoptosis mechanisms
56 involve complex pathway; when in the normal state, the
57 caspase-dependent pathway is main apoptosis pathway; when the caspase
58 is suppressed, the BHK-21 can switch on the caspase-independent
59 pathway by AIF, Endo G, or Mst3 to allow apoptosis to continue.

60

61 **Keywords:** *Newcastle disease virus, Apoptosis, Caspase-independent*
62 *pathway*

63 **Background**

64 Newcastle disease virus (NDV) is a single-stranded, negative-sense,
65 non-segmented RNA genome of the genus *Avulavirus* in the family
66 *Paramyxoviridae* [1]. It is virus with great significance; it has caused
67 more outbreaks than any other virus and has a high lethality in fowl
68 worldwide. However, the virus' oncolytic efficacy is emerging as a novel
69 cancer treatment and may give NDV a new research direction [2-4]. NDV
70 was first used to treat cancer in in the early 1950's; NDV treatment
71 induced tumor apoptosis or partial necrosis and sloughing in uterine
72 carcinoma [5]. In 2013, Shobana et al. altered the viral fusion protein for
73 exclusive cleavage by a prostate-specific antigen, making it the target of a
74 tumor-specific signal for induction of apoptosis [6].

75

76 NDV *in vivo* can induce spleen, thymus, bursa, and mesenteric glands cell
77 apoptosis for immunosuppression [7-9]. Most studies that have focused
78 on apoptosis have determined whether or not it occurred, without further
79 study of the *in vivo* mechanism. In this study, NDV has been discovered
80 as a good oncolytic virus. NDV safely and effectively infects and kills

81 cancer cells. NDV is considered to be a good potential oncolytic agent in
82 a clinical setting and is an experimental oncolytic agent [10]. Researchers
83 have change NDV in vitro to target cancer cell specific markers and were
84 confirmed in HT1080, KHOS, KB8-5011, HCV29T, IMR32, and G104
85 cell lines to cause cell apoptosis and lack of apoptosis in normal cells [5,
86 11, 12].

87

88 Apoptosis is a programmed multistep cell death that is intrinsic in all cells
89 of the body; it is a necessary biological defense mechanism. Apoptosis
90 has two pathways: a cysteine-aspartyl specific protease activation
91 pathway (caspase-dependent) and an inactivated-caspase pathway
92 (caspase-independent) [13]. Most apoptosis occurs because of multiple
93 pathway interactions those that utilize a receptor, enzyme, regulatory
94 protein, and signal transduction molecules. In the apoptosis research, the
95 different cell induce cell death program are difference [14]. The viruses
96 that induce apoptosis have two types. Direct pathways include the
97 caspase-dependent pathway, mitochondria-mediated pathway, death
98 receptor-mediated pathway, endoplasmic reticulum stress pathway, and

99 mitogen-activated protein kinases pathways. Indirect pathways utilize
100 secretion of proinflammatory cytokines and chemokines and induction of
101 the innate and acquired immune responses. The natural killer cells,
102 lymphocytes, and macrophages are then stimulated to remove cells from
103 the diseased area [15].

104

105 In 2006, Elankumaran et al. showed that NDV can use a
106 caspase-dependent pathway for 16 different types of cell apoptosis, the
107 major pathways being the mitochondria-mediated and death
108 receptor-mediated pathway. Interestingly, when caspase is inhibited and
109 cells are treated with NDV, apoptosis can still occur. It appears that NDV
110 can induce apoptosis through a caspase-independent pathway [16]. After
111 this, the other apoptosis pathways investigated were p53, Bax, and p3
112 MAPK during 2009 to 2011 [17-20]. However, no other signals from
113 NDV induce apoptosis a caspase-independent pathway in the cell.
114 Therefore, we wanted to examine the mechanism by which NDV induces
115 cell apoptosis through a caspase-independent pathway and identify the
116 proteins involved in it.

117 **Methods**

118 *Cells and virus*

119 The BHK-21 (baby hamster kidney) cell line was grown in Dulbecco's
120 modified Eagle medium with 10% fetal bovine serum (FBS), 100 U/ml of
121 penicillin and streptomycin at 37°C in a 5% CO₂ humidified incubator.
122 NDV was isolated from a wild strain; after sequencing, it was determined
123 to be *Miyadera* (gbjM 18456.1) and was then amplified. The final sample
124 was quantified at a concentration of 10^{3.8}TCID₅₀/μl, and the virus was
125 stored at -80°C for further use. The samples were divided into two
126 groups for this research; the normal NDV infection group (caspase group)
127 and the caspase inhibition group. The caspase inhibition group was
128 treated with 100μM pan-caspase inhibitor z-VAD-fmk
129 (Z-Val-Ala-DL-Asp-fluoromethylketone) in the culture medium 1 h
130 before virus treatment.

131

132 *DNA fragmentation*

133 The BHK-21 cells at a concentration of 2×10⁶ were infected with an
134 NDV MOI of 1. The samples were separated as caspase and caspase

135 inhibition groups. After the 0, 12, and 24 h of incubation, the detached
136 cells in the medium were collected. The pellet was washed with PBS
137 twice, and lysed with lysis buffer (50 mM Tris-HCl, pH 7.5, 20 mM
138 EDTA, and 1% Nonidet P-40). The supernatant was collected and
139 incubated with RNaseA at a final concentration 5µg/µl for 2 h at 56°C.
140 Proteinase K was added to a final concentration of 2.5 µg/µl, and the
141 mixture was incubated at 37°C for 2 h. Furthermore, 3 M acetic acid (10
142 µl), 20 µl saturated sucrose, and cold 100% ethanol at a 2.5x volume was
143 added, and the sample was stored at -80°C overnight. The sample pellet
144 was collected and washed with cold 80% ethanol. The samples were dried
145 at room temperature for 10 min, dissolved in deionization and distilled
146 water, and diluted to a concentration of 5 µg per well. Finally,
147 electrophoresis was performed using 2% agarose gel.

148

149 *TUNEL assay (Terminal deoxynucleotidyl transferase dUTP nick end*
150 *labeling assay)*

151 The BHK-21 cells were diluted at a concentration of 3×10^5 and infected
152 with NDV MOI of 1. The sample was separated into the caspase and

153 caspase inhibitor groups. After the 0, 12, and 24 h of incubation at 37°C
154 in an atmosphere of 5% CO₂, the TUNEL assay was carried out using a
155 FragEL™ DNA Fragmentation Detection Kit (CALBIOCHEM,
156 QIA33-1EA). The cover slip was sealed with 40% glycerol, and
157 observation and counting were done under a microscope.

158

159 *Western blot analysis*

160 The western blot sample was applied to the two groups of caspase and
161 caspase inhibition at 0, 12, and 24 h. In addition, the samples were
162 differentiated between groups using total protein, cytoplasm protein, and
163 nuclear protein groups at 0 and 24 h. The BHK-21 cells at a concentration
164 of 2×10^6 were infected with an NDV MOI of 1. The cytoplasm protein
165 was extracted using buffer I (10 mM HEPES, 1.5 mM MgCl₂, 10 mM
166 KCl, 0.5 mM OTT, 0.05% NP-40, prepared at pH 7.9) and the other
167 groups were extracted using RIPA lysis buffer. All samples were
168 quantified using a Bio-Rad protein assay reagent with a protein of a
169 uniform weight of 50 µg. All samples were separated by 12% SDS-PAGE
170 and transferred onto a PVDF membrane (Millipore, USA). The

171 membranes were blocked and incubated with antibody with NET buffer
172 (Gelatin 2.5 g, NaCl 8.75 g, DETA·2Na 1.8 g, Tris 6.05 g, Tween 20 0.5
173 ml in 1 L water, pH 8.0). The primary antibody was incubated overnight
174 at 4°C with α -tubulin (SC8035, Santa Cruz Bioechnology, CA), actin
175 (MAB1501, Millipore, USA), AIF (SC1946, Santa Cruz Bioechnology,
176 CA), Bax (SC493, Santa Cruz Bioechnology, CA), Bcl-2 (SC7382, Santa
177 Cruz Bioechnology, CA), cleaved caspase-3 (SC22171, Santa Cruz
178 Bioechnology, CA), cytochrome C (SC7159, Santa Cruz Bioechnology,
179 CA), Endo G (SC26923, Santa Cruz Bioechnology, CA), GADPH
180 (ab9483, Abcam[®], UK), lamin B (SC6216, Santa Cruz Bioechnology,
181 CA), Mst3 (SC21400, Santa Cruz Bioechnology, CA), and NDV
182 (ab138719, Abcam[®], UK). After washing, horseradish peroxidase
183 (HRP)-conjugated secondary antibodies were added and the abundance of
184 proteins was quantified via chemiluminescence assay using an ECL kit
185 (WBULS0500, Millipore, USA). The image was acquired using an
186 illumination imaging system (UVP, Upland, CA, USA) and the amount
187 of proteins was estimated via densitometric analysis using the
188 Bio-imaging camera system. The quantity of each protein was calculated

189 according to the GAPDH detected in each sample. The relative
190 abundance of each protein was determined by dividing the arbitrary unit
191 over that of their 0 h protein.

192

193 *Immunofluorescence*

194 The BHK-21 cells at a concentration of 3×10^5 and infected with an
195 NDV MOI of 1. The cells were challenged with NDV at 0 and 24 h, the
196 caspase and caspase inhibitor groups were incubated separately. The
197 sample was added to Mitotracker (Invitrogen, M-7512) (50 $\mu\text{g}/\text{mL}$) and
198 incubated at 37°C for 30 min, after which the medium was removed and
199 the cover slip was washed with cold PBST. After that, the cells were
200 fixed with 3.7% ice-cold paraformaldehyde for 10 min. Following, the
201 slip washed three times with cold PBST. The sample was added to the
202 primary antibodies (goat anti-AIF and goat anti-Endo G Santa Cruz, USA;
203 chicken anti-ND Abcam[®], UK) in PBST for at least 4 h at room
204 temperature. After washing, the cells were incubated with
205 FITC-conjugated donkey anti-goat IgG (Santa Cruz, USA) or goat
206 anti-chicken IgY (Santa Cruz, USA) in PBST at room temperature for 1 h

207 in the dark. Then, the cells were added to DAPI 1 $\mu\text{g}/\mu\text{L}$ in PBST at
208 room temperature for 25 min in the dark. Finally, the cells were placed
209 under the cover slip sealed with 40% glycerol, and visualization was
210 carried out using a fluorescence microscope.

211

212 **Results**

213 *Induction of apoptosis by NDV-mediated caspase and*
214 *caspase-independent pathway in BHK-21 cells*

215 The NDV-treated BHK-21 cells had been divided into two groups, one
216 group was directly challenge by NDV, and the other group was treated
217 with pan-caspase inhibitor z-VAD-fmk (final concentration 100 μM) to
218 inhibit caspase-dependent pathway apoptosis before challenged with
219 NDV. Cell apoptosis was induced by a caspase-dependent pathway with
220 activation of caspase-3 by entering the nuclei; the caspase protein will cut
221 the DNA according to nucleosome nucleotides length, causing DNA
222 fragmentation. In Figure 1a, the caspase group indicated that the caspase
223 family protein cut the DNA according to nucleosome nucleotides length
224 that became the DNA markers in the 2% agarose gel. The caspase

225 inhibition group did not take the shape of DNA ladders after NDV
226 infection, as the caspase group did (Figure 1b). The rate of cell apoptosis
227 and cells fusion increased as time passed. The ratios of apoptosis of the
228 caspase group from 0, 12, and 24 h were $6.50 \pm 1.69\%$, $29.59 \pm 3.52\%$,
229 and $62.48 \pm 3.69\%$, respectively. On the other hand, for the caspase
230 inhibitor group, the apoptosis ratios from 0, 12, and 24 h were $5.94 \pm$
231 0.75% , $22.92 \pm 1.66\%$, $32.57 \pm 1.31\%$, respectively. The data are shown
232 in Figure 3a–g. In addition, we observed that NDV infection increased
233 cell fusion depending on the infection time. The ratios of cell fusion of
234 caspase group at 0, 12, and 24 h were $0 \pm 0\%$, $7.15 \pm 1.32\%$, and $35.81 \pm$
235 3.53% , respectively, and in caspase inhibitor group, the ratios of cell
236 fusion at 0, 12, and 24 h were $0 \pm 0\%$, $4.85 \pm 2.77\%$, and $17.55 \pm 1.84\%$,
237 respectively (Fig 2h).

238

239 *NDV mediates BHK-21 cell apoptosis caspase-dependent and*
240 *-independent pathway.*

241 NDV induced apoptosis via caspase-dependent and caspase-independent
242 pathways in BHK-21 cells. In the two groups, we used 0 h protein as a

243 starting point to confirm protein expression at 12 and 24 h. The results
244 reveal that the proapoptotic proteins Bax, cytochrome C, Mst3, and AIF
245 were increased over time and the antiapoptotic protein Bcl-2 decreased
246 over time, regardless of the caspase-dependent or -independent pathway.
247 Among them, Endo G was special; it was increased at 24 h in the
248 caspase-dependent pathway and increased over time in the
249 caspase-independent pathway; however, only the cleaved caspase-3 was
250 different. It was inhibited by z-VAD-fmk in the caspase-independent
251 pathway. In addition to apoptosis, we found that NDV-treated BHK-21
252 cells had less actin, regardless of having caspase or not. The actin always
253 decreased in the NDV-treated BHK-21 cells at 12 and 24 h. This was
254 because we used GAPDH to do protein internal control, not used actin.
255 The western blot data were shown in Figure. 3.

256

257 *In apoptosis caspase-independent pathway, Mst3, AIF, and Endo G are*
258 *transferred from the mitochondria to the nucleus*

259 In Figure 4a and 4b, the sample was separated it two groups; one was
260 caspase apoptosis group that had 0 h total protein (0 h T), 0 h cytoplasmic

261 protein (0 h C), 0 h nucleus protein (0 h N), 24 h total protein (24 h T), 24
262 h cytoplasmic protein (24 h C), and 24 h nucleus protein (24 h N). The
263 other group were caspase inhibited group that had same protein samples.
264 The total protein internal control was actin, the cytoplasmic protein
265 sample was α -tubulin, and the nucleus protein sample was lamin B. In
266 Figure 4a, we confirm the transfer of Mst3, AIF, and Endo G from
267 cytoplasm to the nucleus; Figure 4b shows that the caspase inhibition
268 group was similar to the caspase group in terms of current protein
269 expression. After that, we showed the image data in immunofluorescent
270 staining in Figure 5a and 5b. In Figure 5a and 5b, the green color is target
271 protein (FITC), red color is mitochondria (Mitoracker), and blue marks
272 the nucleus (DAPI). The FITC three different target proteins were AIF,
273 Endo G, and NDV. In Figure 5a and 5b, the 0 h, all samples show the
274 protein of AIF and Endo G in cytoplasmic, and the color overlaps appear
275 yellow. AIF and Endo G are transferred from the mitochondria to the
276 nucleus 24 h after NDV infection. NDV replicated in cell cytoplasm and
277 induced cell aggregation and fusion.
278

279 **Discussion**

280 NDV infect BHK-21 for 24 h caused growth inhibition in MMT assay. At
281 36 h, the MTT illustrated negative growth but this cannot explain how
282 NDV can induce BHK-21 cell apoptosis, let alone through an apoptotic
283 pathway. The findings must be confirmed by more specific experiments,
284 like DNA fragmentation and TUNEL assay. When caspase-dependent
285 pathway would be inhibited, NDV can induce BHK-21 apoptosis by
286 caspase-independent pathway (Figure 3). In the tests, we used NDV
287 added to BHK-21 cell before treatment with caspase inhibitor
288 z-VAD-fmk to control caspase-dependent or independent pathway. NDV
289 induced BHK-21 apoptosis via caspase-dependent and
290 caspase-independent pathways (Figure 3). This result is the same as that
291 obtained with THP-1, leukemia cell lines, HL cells, and HEG2 cell lines
292 treated with NDV [15, 16].

293 Studies on the pathways of apoptosis induction in specific cells by NDV
294 can cause different cells to undergo apoptosis in different pathways. Most
295 NDV apoptosis papers showed that both the extrinsic and intrinsic
296 pathways are activated in NDV-induced apoptosis. In 2011 the paper

297 confirmed that PC12 rat pheochromocytoma cell mitogen-activated
298 protein kinase pathway was not involved in NDV-induced apoptosis, but
299 in A549 human lung cancer, can induce apoptosis using the p38 and
300 MAPK pathway, in addition, the endoplasmic reticulum apoptosis
301 pathway no effect [17, 20]. When NDV induces cell apoptosis, Bax
302 transfers from cytoplasm to mitochondria and cytochrome C transfers
303 from mitochondria to cytoplasm. But Bcl-2 of protein expression is not
304 any increase and decrease in NDV-induced apoptosis. If the caspase
305 would be suppressed, the cell would be induced caspase-independent
306 apoptosis pathway [16, 18, 21]. In summary, NDV-induced apoptosis has
307 two mechanisms; one is NDV has different apoptosis pathways induced
308 by different cells, and there is no absolute path followed. The other is
309 NDV-induced apoptosis is a complex multiple pathway response. Our
310 study showed that cytochrome C, AIF, Mst3, and Endo G were important
311 because their proteins express increasingly from 0 to 24 h. Bax in
312 caspase-dependent or independent pathway is increase protein expression,
313 but the Bcl-2 is decrease.

314

315 The Bax protein configuration changes and aggregation can promote
316 apoptosis; Bcl-2 can prevent that when the Bcl-2 protein expressed more
317 than Bax and there is no apoptosis [22-25]. His study of NDV-induced
318 HeLa cell apoptosis showed that Bax configuration changed before NDV
319 infected the cell and that the Bax protein changed location and caused
320 cytochrome C from the mitochondria to be released into the cytoplasm;
321 the activity of Bcl-2 remained unchanged [18]. We observed the state of
322 the Bax and the Bcl-2 was different. The Bax continued to increase with
323 or without added inhibitors and Bcl-2 was exactly the opposite in our
324 study. Expression of the other proteins Mst3, AIF, Endo G, and
325 cytochrome C protein increased over time. Bax is an upstream regulatory
326 protein in apoptosis that mainly affects the release of apoptotic proteins in
327 the mitochondria and ultimately promotes the release of Endo G, AIF,
328 and cytochrome C from the mitochondria, in which immunofluorescence
329 staining results show that AIF and Endo G are two apoptotic proteins that
330 are transferred to the nucleus because of NDV infection of BHK-21 cells.
331
332 During NDV infection, the cell surface often accumulates highly fused F

333 protein implants into infected cells to form a multinucleate state to
334 facilitate virus transmission [26]. This phenomenon can be easily
335 identified using a TUNEL assay and immunofluorescence, and the state
336 of cell fusion has also been shown to effectively enhance NDV-induced
337 cancer cell apoptosis in vitro or in vivo. How did the cell structure change
338 affect our experiment? In the case of BHK-21 infected with NDV, the
339 most special change was actin. Originally in 1977, NDV infection of
340 BHK-21 was mentioned in a paper that actin will change with the
341 infection. The paper uses immunofluorescence light staining to mark
342 actin, and the results showed that actin has an increasing trend after
343 adding virus [27]. However, the results of our experiment show that the
344 actual performance of actin is declining, because the 1977 paper did not
345 use western blotting and other more accurate protein detection methods to
346 confirm; NDV can promote the infection of cells *in vitro* to cause cell
347 fusion. When multiple cells are aggregated into one, the amount of actin
348 should higher than that of a single cell. Actin is one of the cytoskeletal
349 proteins in cells. Actin is involved in the various processes of virus
350 infection, assembly, and release. Among the viruses of the

351 *Paramyxoviridae* family, actin is involved in the viral fusion protein (F
352 protein). In the case of the matrix protein (M protein), when a large
353 amount of F protein appears on the surface of the host cell, it will initiate
354 the cell fusion between cells, and the M protein will transport the F
355 protein and HN protein to the assembly process. The inner side of the cell
356 membrane is fixed, and the fixation process also requires the participation
357 of actin [27-30]. Actin will also be affected by caspase. When the cell
358 breaks down, caspase-3, -6, and -9 can directly cleave poly (ADP-ribose)
359 polymerase-1 (PARP), lamins, CAD, and actin, which may explain the
360 lower actin content over time, coupled with cell fusion and various effects
361 of virus assembly. This results in decreased actin protein content in
362 BHK-21 cells after 24 h following challenge with NDV; the content is
363 reduced to 0.60 times of 0 h.

364

365 **Conclusions**

366 In this study, we show the NDV-mediated BHK-21 cell apoptosis
367 mechanisms involve complex pathway; when in the normal state, the
368 caspase-dependent pathway is main apoptosis pathway; when the caspase
369 is suppressed, the BHK-21 can switch on the caspase-independent

370 pathway by AIF, Endo G, or Mst3 to allow apoptosis to continue. And
371 actin will also be affected by caspase, which may explain the lower actin
372 content over time.

373

374 **List of abbreviations**

375 NDV Newcastle disease virus

376 BHK Baby hamster kidney

377 z-VAD-fmk Z-Val-Ala-DL- Asp-fluoromethylketone

378 caspase cysteine aspartyl specific proteases

379

380 **Declarations**

381 **Ethics approval and consent to participate:** Not applicable.

382 **Consent for publication:** Not applicable.

383 **Availability of data and materials:** All relevant data are within the
384 paper and its Supporting Information files.

385 **Funding:** The authors received no specific funding for this work.

386 **Conflict of Interest:** The authors declare no conflicts of interest.

387 **Authors' contributions:** Conceptualization: Wang CW, Wu HY; Data
388 curation: Wang CW, Wu HY; Formal analysis: Wang CW, Wu HY , Lin

389 CY; Funding acquisition: Wu HY; Investigation: Wang CW, Wu HY;
390 Methodology: Wang CW, Shih WL, Wu HY; Project administration:
391 Wang CW, Wu HY; Resources: Wu HY; Software: Wang CW;
392 Supervision: Wang CW, Lin CY, Wu HY; Validation: Wang CW,
393 Thongchan D; Chung SC, Lin TC, Wu HY; Visualization: Wang CW,
394 Wu HY; Writing-original draft: Wang CW, Wu HY; Writing-review &
395 editing: Wang CW, Wu HY

396 **Acknowledgements** : The authors would like to acknowledge the
397 excellent technical assistance provided by Chiun Jye Yuan, Guan Ming
398 Ke, Yen Li Huang, Wei Lin, Hung Li ,Pei Ting Deng . We also thank the
399 Nano Biology and Biosensing Lab, National Yang Ming Chiao Tung
400 University.

401 **Authors' information** : Chen-Wei Wang¹, Chia-Ying Lin², Sheng-Chang
402 Chung¹, Wen-Ling Shih³, Tzu-Chieh Lin⁴, Duangsuda Thongchan⁵,
403 Hung-Yi Wu^{1*}

404 1. Department of Veterinary Medicine, College of Veterinary
405 Medicine, National Pingtung University of Science and Technology,
406 No.1, Shuefu Rd., Neipu, Pingtung 91201, Taiwan.

- 407 2. Da Dian Biotechnology Company Limited, No. 21, Aly. 22, Ln. 77,
408 Hengnan Rd., Hengchun Township, Pingtung County 946001,
409 Taiwan
- 410 3. Department of Biological Science and Technology, National
411 Pingtung University of Science and Technology, No.1, Shuefu Rd.,
412 Neipu, Pingtung 91201, Taiwan.
- 413 4. International Degree Program in Animal Vaccine Technology,
414 National Pingtung University of Science and Technology, No.1,
415 Shuefu Rd., Neipu, Pingtung 91201, Taiwan.
- 416 5. Faculty of Agriculture and Technology, Rajamangala University of
417 Technology Isan, Surin campus, 145 Moo 15 Surin-Prasat Road,
418 Nokmuang, Muang District, Surin Province, Thailand, 32000

419

420 **References**

- 421 1. Mayo MA. A summary of taxonomic changes recently approved by
422 ICTV. Arch Virol. 2002;147(8):1655-63. doi:
423 10.1007/s007050200039, PMID 12181683.
- 424 2. Southam CM, Hilleman MR, Werner JH. Pathogenicity and oncolytic
425 capacity of RI virus strain RI-67 in man. Lab Clin Med.

- 426 1956;47(4):573-82. PMID 13307092.
- 427 3. Southam CM, Moore AE. Clinical studies of viruses as antineoplastic
428 agents with particular reference to Egypt 101 virus. *Cancer*.
429 1952;5(5):1025-34. doi:
430 10.1002/1097-0142(195209)5:5<1025::aid-cnrcr2820050518>3.0.co;2-
431 q, PMID 12988191.
- 432 4. Okuno Y, Asada T, Yamanishi K, Otsuka T, Takahashi M, Tanioka T,
433 Aoyama H, Fukui O, Matsumoto K, Uemura F, Wada A. Studies on
434 the use of mumps virus for treatment of human cancer. *Biken J*.
435 1978;21(2):37-49. PMID 749908.
- 436 5. Lam HY, Yeap SK, Pirozyan MR, Omar AR, Yusoff K, Suraini AA,
437 Abd-Aziz Suraini, Alitheen NB. Safety and clinical usage of
438 Newcastle disease virus in cancer therapy. *J Biomed Biotechnol*.
439 2011;2011:718710. doi: 10.1155/2011/718710.
- 440 6. Shobana R, Samal SK, Elankumaran S. Prostate-specific
441 antigen-retargeted recombinant Newcastle disease virus for prostate
442 cancer virotherapy. *J Virol*. 2013;87(7):3792-800. doi:
443 10.1128/JVI.02394-12, PMID 23345509.

- 444 7. Anis Z, Morita T, Azuma K, Ito H, Ito T, Shimada A.
445 Histopathological alterations in immune organs of chickens and ducks
446 after experimental infection with virulent 9a5b Newcastle disease
447 virus. *J Comp Pathol.* 2013;149(1):82-93. doi:
448 10.1016/j.jcpa.2012.09.011, PMID 23369809.
- 449 8. Harrison L, Brown C, Afonso C, Zhang J, Susta L. Early occurrence
450 of apoptosis in lymphoid tissues from chickens infected with strains of
451 Newcastle disease virus of varying virulence. *J Comp Pathol.*
452 2011;145(4):327-35. doi: 10.1016/j.jcpa.2011.03.005, PMID
453 21511269.
- 454 9. Hu Z, Hu J, Hu S, Liu X, Wang X, Zhu J, Liu X. Strong innate
455 immune response and cell death in chicken splenocytes infected with
456 genotype VIIId Newcastle disease virus. *Virology* 2012;9:208. doi:
457 10.1186/1743-422X-9-208, PMID 22988907.
- 458 10. Csatory LK. Viruses in the treatment of cancer. *Lancet.*
459 1971;2(7728):825. doi: 10.1016/s0140-6736(71)92788-7, PMID
460 4106650.
- 461 11. Apostolidis L, Schirmacher V, Fournier P. Host mediated anti-tumor

462 effect of oncolytic Newcastle disease virus after locoregional
463 application. Int J Oncol. 2007;31(5):1009-19. PMID 17912426.

464 12.Sánchez-Felipe L, Villar E, Muñoz-Barroso I. Entry of Newcastle
465 disease virus into the host cell: role of acidic pH and endocytosis.
466 Biochim Biophys Acta. 2014;1838(1 Pt B):300-9. doi:
467 10.1016/j.bbamem.2013.08.008, PMID 23994097.

468 13.Donovan M, Cotter TG. Control of mitochondrial integrity by Bcl-2
469 family members and caspase-independent cell death. Biochim
470 Biophys Acta. 2004;1644(2-3):133-47. doi:
471 10.1016/j.bbamcr.2003.08.011, PMID 14996498.

472 14.Horvitz HR. Genetic control of programmed cell death in the
473 nematode *Caenorhabditis elegans*. Cancer Res.
474 1999;59(7);Suppl:1701s-6s. PMID 10197583.

475 15.Zamarin D, Palese P. Oncolytic Newcastle disease virus for cancer
476 therapy: old challenges and new directions. Future Microbiol.
477 2012;7(3):347-67. doi: 10.2217/fmb.12.4, PMID 22393889.

478 16.Elankumaran S, Rockemann D, Samal SK. Newcastle disease virus
479 exerts oncolysis by both intrinsic and extrinsic caspase-dependent

480 pathways of cell death. *J Virol.* 2006;80(15):7522-34. doi:
481 10.1128/JVI.00241-06, PMID 16840332.

482 17.Bian J, Wang K, Kong X, Liu H, Chen F, Hu M, Zhang X, Jiao X, Ge
483 B, Wu Y, Meng S. Caspase- and p38-MAPK-dependent induction of
484 apoptosis in A549 lung cancer cells by Newcastle disease virus. *Arch*
485 *Virol.* 2011;156(8):1335-44. doi: 10.1007/s00705-011-0987-y, PMID
486 21625975.

487 18.Molouki A, Hsu YT, Jahanshiri F, Rosli R, Yusoff K. Newcastle
488 disease virus infection promotes Bax redistribution to mitochondria
489 and cell death in HeLa cells. *Intervirology.* 2010;53(2):87-94. doi:
490 10.1159/000264198, PMID 19955813.

491 19.Ravindra PV, Tiwari AK, Ratta B, Bais MV, Chaturvedi U, Palia SK,
492 Sharma B, Chauhan RS. Time course of Newcastle disease
493 virus-induced apoptotic pathways. *Virus Res.* 2009;144(1-2):350-4.
494 doi: 10.1016/j.virusres.2009.05.012, PMID 19501124.

495 20.Szeberényi J, Fábíán Z, Töröcsik B, Kiss K, Csatory LK. Newcastle
496 disease virus-induced apoptosis in PC12 pheochromocytoma cells.
497 *Am J Ther.* 2003;10(4):282-8. doi:

498 10.1097/00045391-200307000-00008, PMID 12845392.

499 21.Aguilar HC, Henderson BA, Zamora JL, Johnston GP. Paramyxovirus
500 glycoproteins and the membrane fusion process. *Curr Clin Microbiol*
501 *Rep.* 2016;3(3):142-54. doi: 10.1007/s40588-016-0040-8, PMID
502 28138419.

503 22.Ravindra PV, Tiwari AK, Ratta B, Chaturvedi U, Palia SK, Chauhan
504 RS. Newcastle disease virus-induced cytopathic effect in infected cells
505 is caused by apoptosis. *Virus Res.* 2009;141(1):13-20. doi:
506 10.1016/j.virusres.2008.12.008, PMID 19152817.

507 23.Dlugosz PJ, Billen LP, Annis MG, Zhu W, Zhang Z, Lin J, Leber B,
508 Andrews DW. Bcl-2 changes conformation to inhibit Bax
509 oligomerization. *EMBO J.* 2006;25(11):2287-96. doi:
510 10.1038/sj.emboj.7601126, PMID 16642033.

511 24.Gross A, Jockel J, Wei MC, Korsmeyer SJ. Enforced dimerization of
512 BAX results in its translocation, mitochondrial dysfunction and
513 apoptosis. *EMBO J.* 1998;17(14):3878-85. doi:
514 10.1093/emboj/17.14.3878, PMID 9670005.

515 25.Nechushtan A, Smith CL, Hsu YT, Youle RJ. Conformation of the

516 Bax C-terminus regulates subcellular location and cell death. *EMBO J.*
517 1999;18(9):2330-41. doi: 10.1093/emboj/18.9.2330, PMID 10228148.

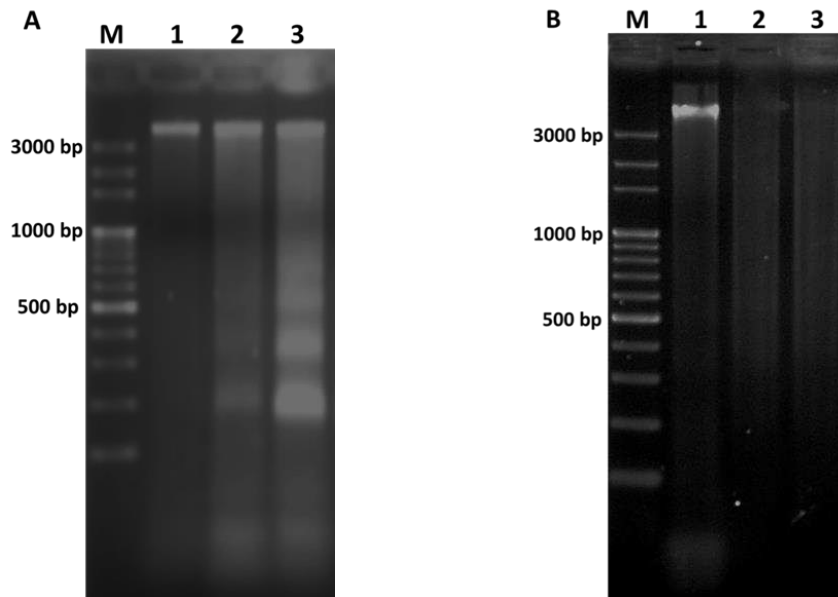
518 26. Wolter KG, Hsu YT, Smith CL, Nechushtan A, Xi XG, Youle RJ.
519 Movement of Bax from the cytosol to mitochondria during apoptosis.
520 *J Cell Biol.* 1997;139(5):1281-92. doi: 10.1083/jcb.139.5.1281, PMID
521 9382873.

522 27. Rutter G, Mannweiler K. Alterations of actin-containing structures in
523 BHK21 cells infected with Newcastle disease virus and vesicular
524 stomatitis virus. *J Gen Virol.* 1977;37(2):233-42. doi:
525 10.1099/0022-1317-37-2-233, PMID 200706.

526 28. Shaikh FY, Utley TJ, Craven RE, Rogers MC, Lapierre LA,
527 Goldenring JR, Crowe JE, Jr. Respiratory syncytial virus assembles
528 into structured filamentous virion particles independently of host
529 cytoskeleton and related proteins. *PLOS ONE.* 2012;7(7):e40826. doi:
530 10.1371/journal.pone.0040826, PMID 22808269.

531 29. Taylor MP, Koyuncu OO, Enquist LW. Subversion of the actin
532 cytoskeleton during viral infection. *Nat Rev Microbiol.*
533 2011;9(6):427-39. doi: 10.1038/nrmicro2574, PMID 21522191.

534 30. Wakimoto H, Shimodo M, Satoh Y, Kitagawa Y, Takeuchi K, Gotoh
535 B, Itoh M. F-actin modulates measles virus cell-cell fusion and
536 assembly by altering the interaction between the matrix protein and
537 the cytoplasmic tail of hemagglutinin. *J Virol.* 2013;87(4):1974-84.
538 doi: 10.1128/JVI.02371-12, PMID 23221571.
539



540

541 Figure 1. The 2% gel electrophoresis of genomic DNA from BHK-21 cell

542 challenged with NDV. M is the 100 bp marker. Lanes 1, 2, and 3

543 represent the extraction time of DNA at 0, 12, and 24 h after NDV

544 challenge. Figure 1a shows the caspase group and 1b shows the caspase

545 inhibition group.

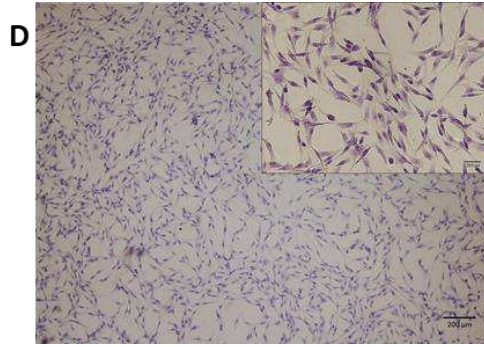
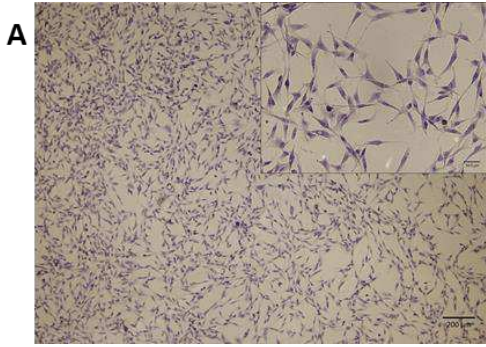
546

547

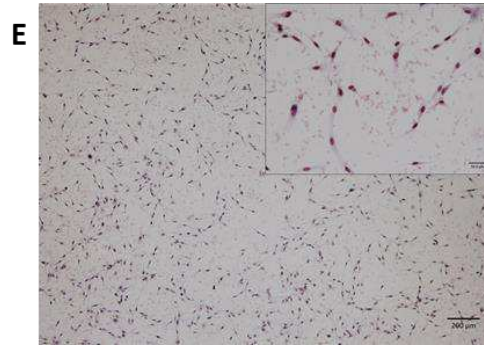
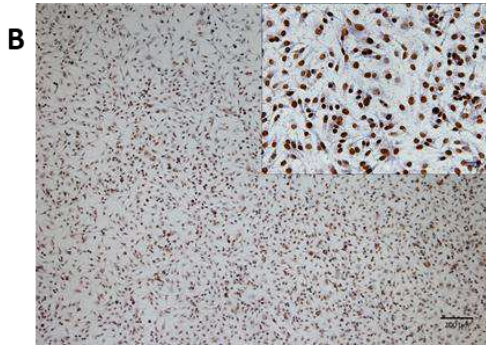
548

549

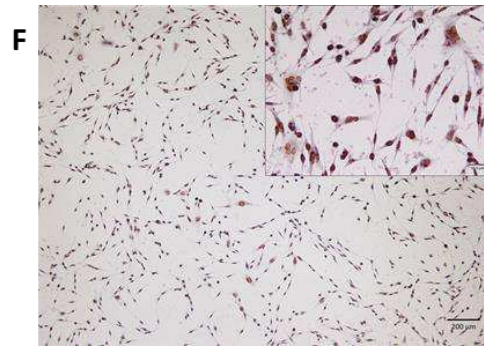
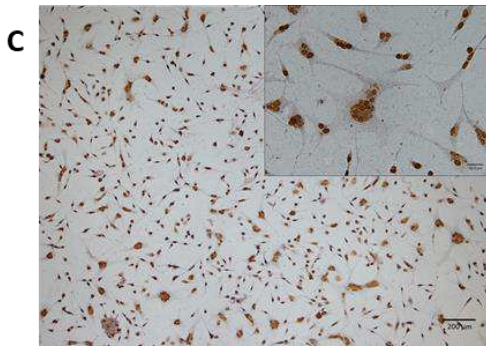
550



551

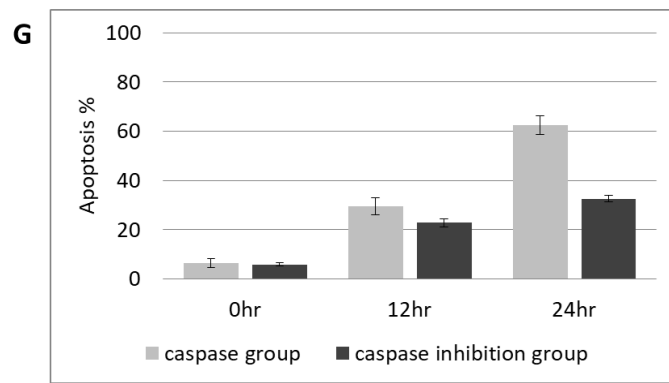


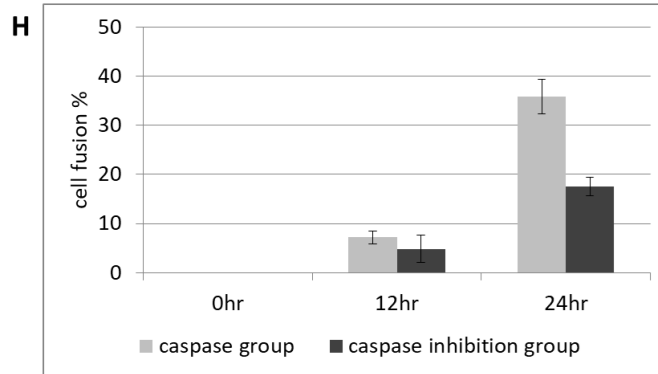
552



553

554





555

556 Figure 2a – f. Microscopic views of two groups of BHK-21 cells after
 557 NDV challenged for 0, 12, and 24 h; samples were treated with
 558 TdT-FragEL™ DNA Fragmentation Detection Kit, and cells with nuclear
 559 showing brownish color are undergoing apoptosis, while the cells with
 560 blue nuclear are living cells. 2a–2c are images of the caspase group and
 561 2D–2F are images of the caspase inhibition group. Figure 2a – 2f is
 562 magnified, scale bar = 200.0 μm (big) and scale bar = 50.0 μm (small).

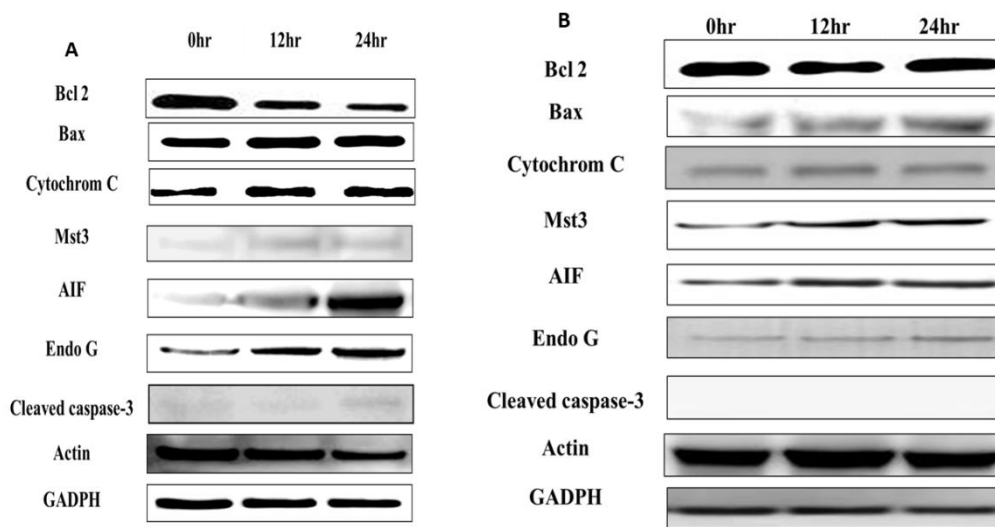
563 2g and 2h. The trend of apoptosis rate in two groups of BHK-21 cells
 564 under different time periods of NDV challenge, the increasing tendency
 565 of apoptosis and cell fusion with or without addition of caspase inhibitor
 566 z-VAD-fmk is confirmed by TUNEL assay. Figure 2g x-axis represents
 567 time after NDV challenge while y-axis is percentage of cells undergoing
 568 apoptosis. Results are shown in the form of mean value ± SD for the three
 569 experiments. Figure 2h is the x-axis representing time after NDV

570 challenge while y-axis stands for percentage of cell undergoing fusion.

571 The results are shown in the form of mean value \pm SD for the three

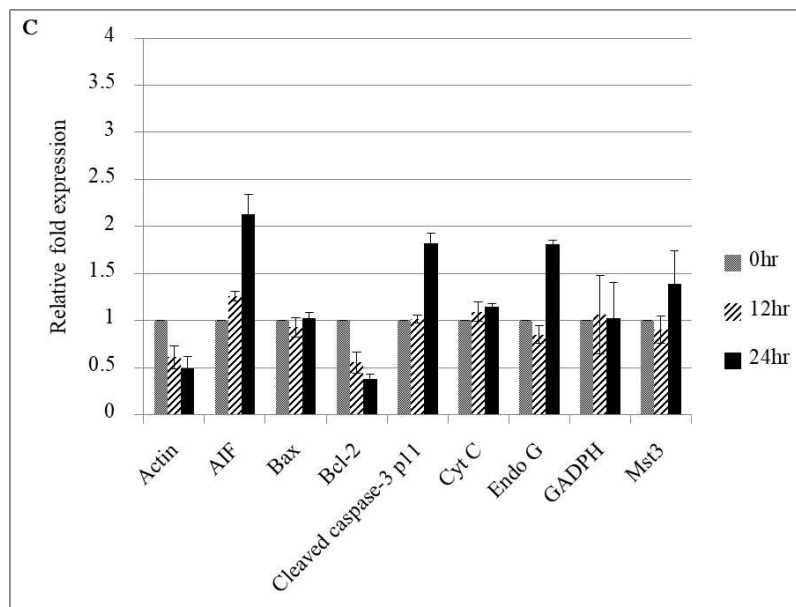
572 experiments.

573

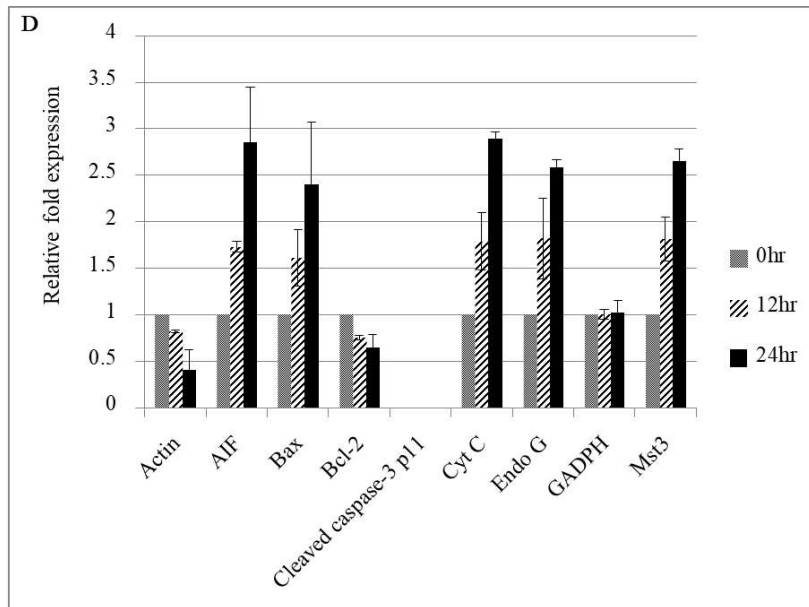


574

575



576



577

578 Figure 3 Influence of the expression of apoptosis-associated proteins at
 579 different times in BHK-21 cells treated with NDV and the caspase
 580 inhibitor z-VAD-fmk at the final concentration of 100 μ M. The proteins
 581 detected were the proapoptotic proteins Bax, cytochrome C, Mst3, AIF,
 582 Endo G, and cleaved caspase-3, the antiapoptotic protein Bcl-2, internal
 583 control GADPH, and actin.

584 (3a) After BHK-21 treatment with NDV for 0, 12, and 24 h, the
 585 caspase-dependent apoptosis-associated proteins were expression.

586 (3b) After BHK-21 treatment with NDV for 0, 12, and 24 h, the
 587 caspase-independent apoptosis-associated proteins were expression.

588 (3c) The graph represents protein expression in the caspase-dependent
 589 group. The x-axis represents apoptosis-associated proteins and the y-axis

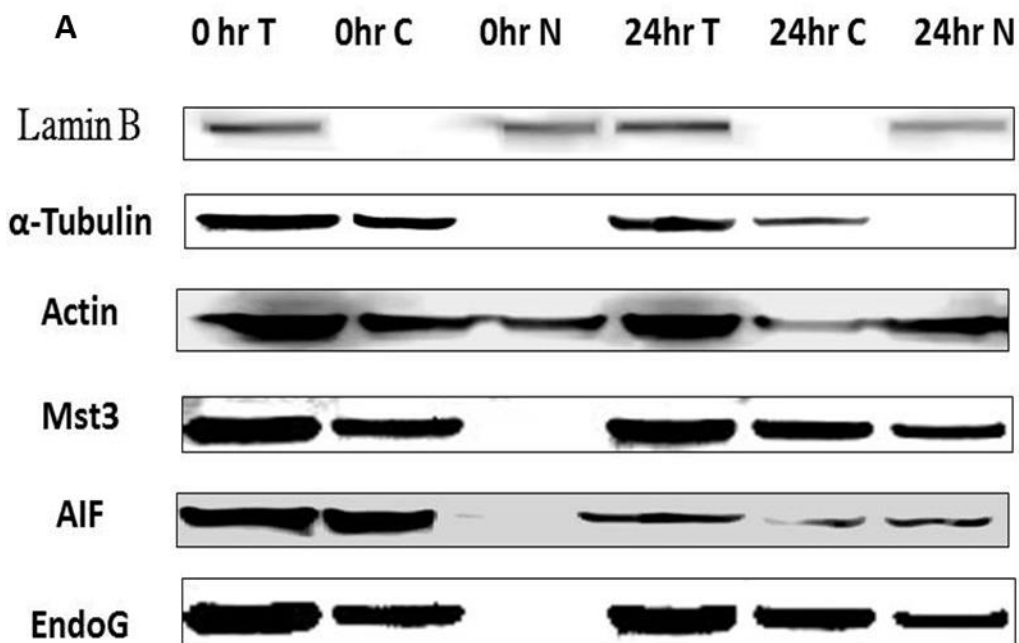
590 represents the relative fold expression, challenge time as 0, 12, and 24 h.

591 (3d) The graph represents protein expression in the caspase inhibition

592 group. The x-axis represents apoptosis-associated proteins and the y-axis

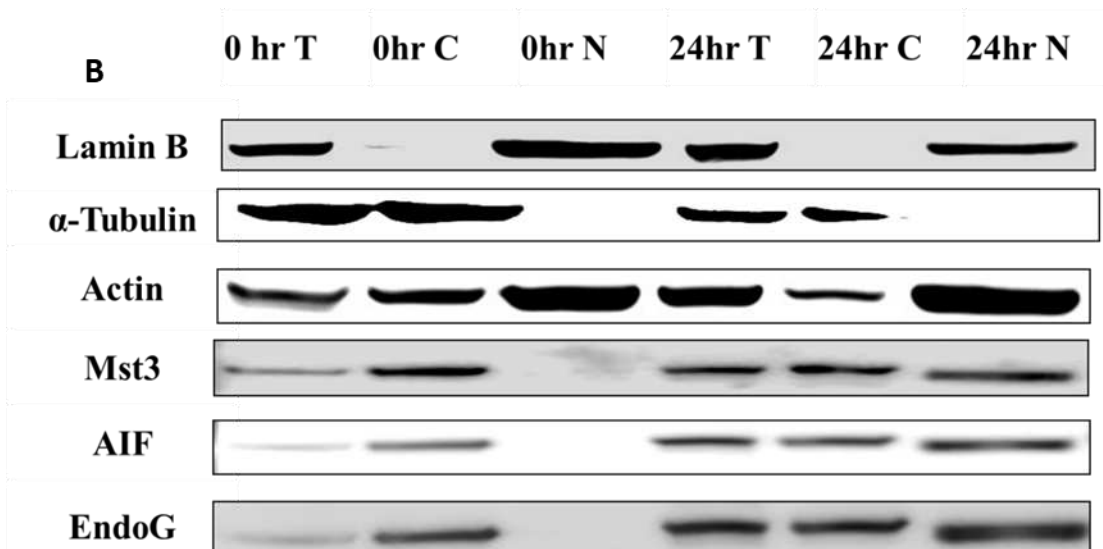
593 represents the relative fold expression, challenge time as 0, 12, and 24 h.

594



595

596



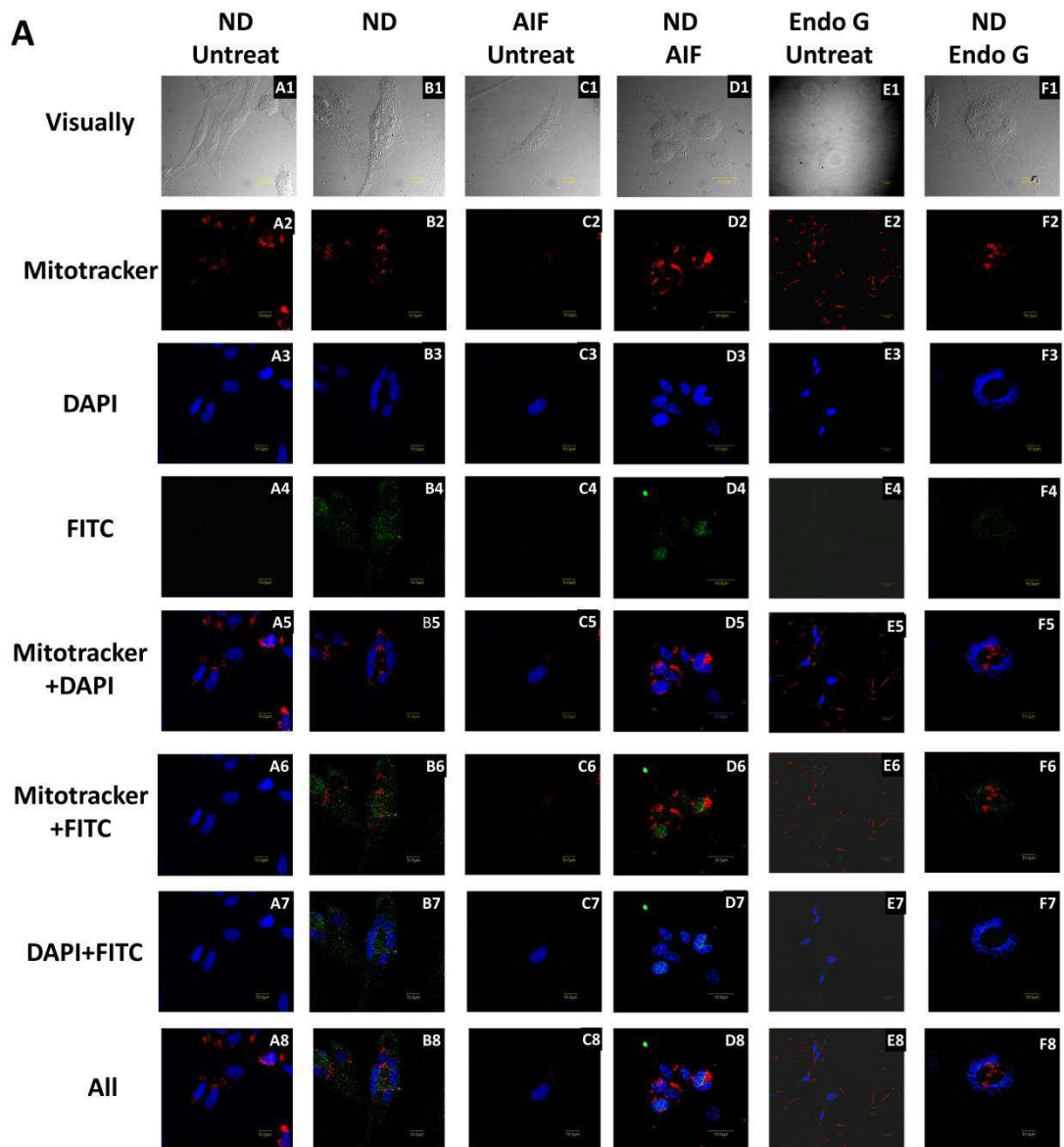
597

598 Figure 4 The cytoplasm and nucleus are shown separately to depict the
599 changes in the positions of proteins. Lamin B is the internal control for
600 the nuclear fraction, α -tubulin is the internal control for the cytoplasmic
601 fraction, and actin is the internal control for the total cell. T: total protein;
602 C: cytoplasmic protein; N: nucleus protein.

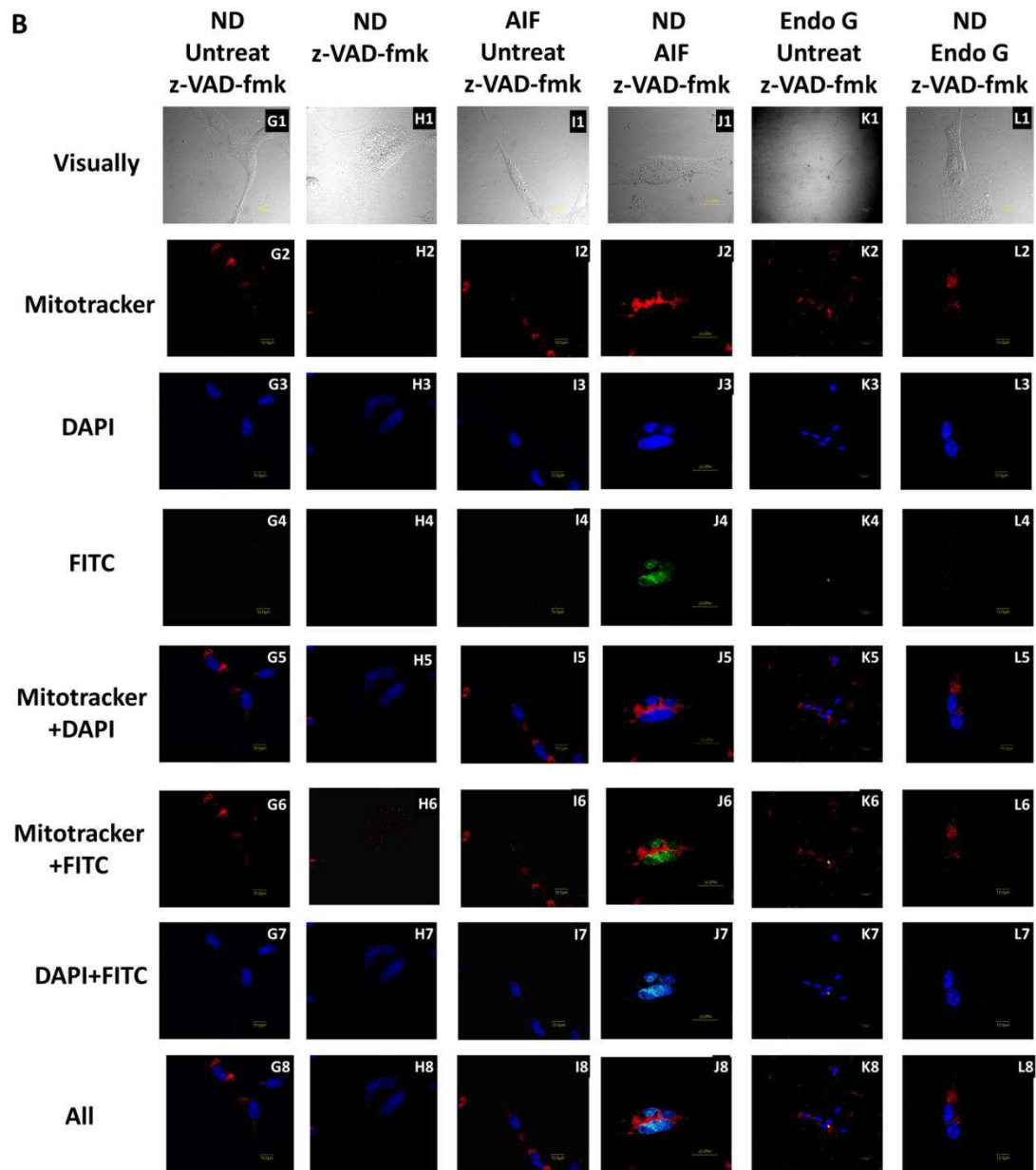
603 (4a) NDV challenged BHK-21 cells at 0 and 24 h (caspase group). Mst3,
604 AIF, and Endo G were transferred from the cytoplasm to the nucleus in
605 the cells.

606 (4b) NDV challenged BHK-21 cells at 0 and 24 h (caspase inhibition
607 group). The Mst3, AIF, and Endo G proapoptotic proteins were similar to
608 those in the caspase group, which help in performing apoptosis in
609 BHK-21 cells.

610



611



612

613

Figure 5 The Endo G and AIF were transferred from the cytoplasm to

614

the nucleus. The green color represents NDV, Endo G, and AIF

615

(FITC). The red color represents the mitochondria (Mitracker). The

616

blue color represents the nucleus (DAPI). (5aA) The BHK-21 was

617

treated NDV 0 and 24 h in apoptosis caspase-dependent study. (5bB)

618

The BHK-21 was treated NDV 0 and 24 h in apoptosis

619 caspase-independent study.

Figures

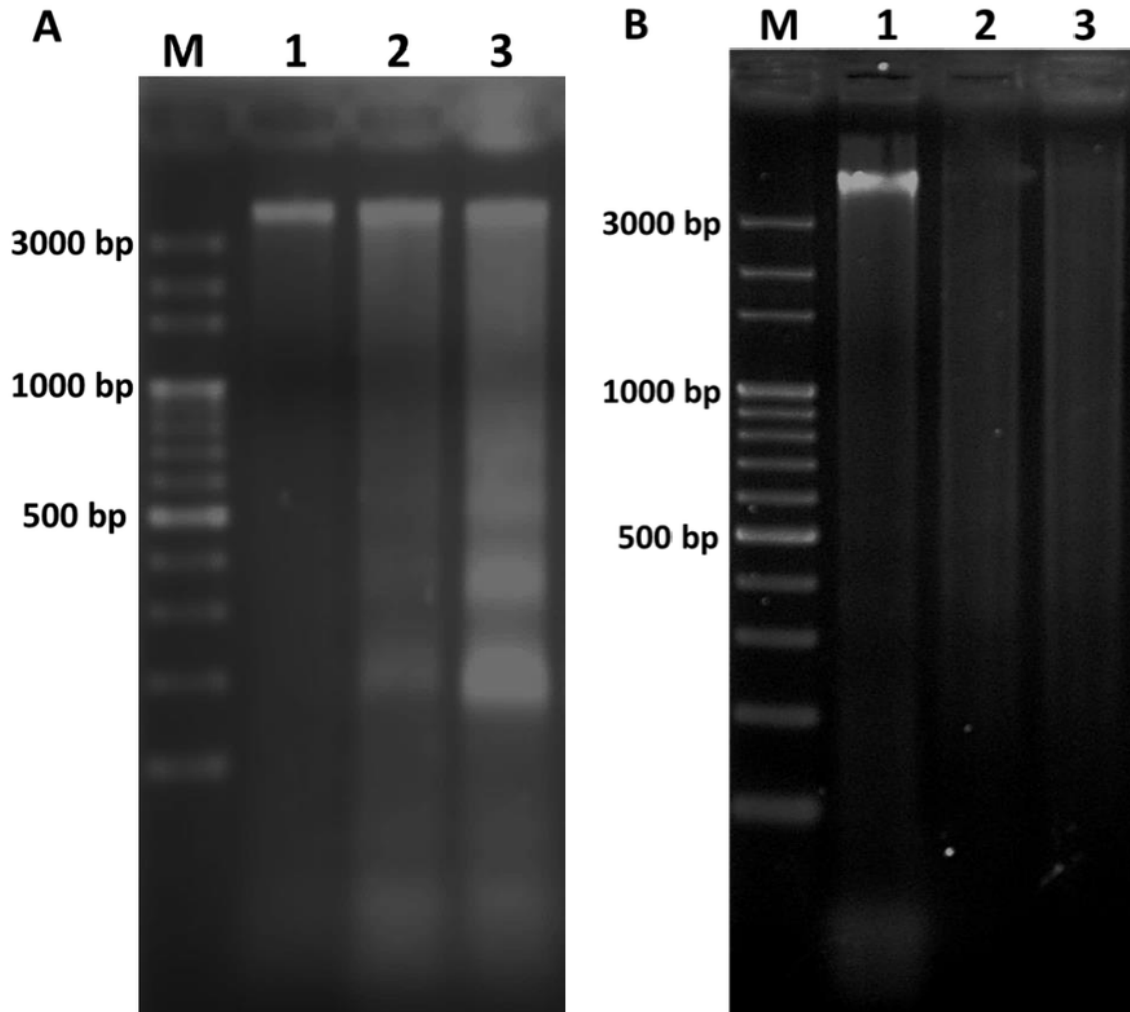


Figure 1

The 2% gel electrophoresis of genomic DNA from BHK-21 cell challenged with NDV. M is the 100 bp marker. Lanes 1, 2, and 3 represent the extraction time of DNA at 0, 12, and 24 h after NDV challenge. Figure 1a shows the caspase group and 1b shows the caspase inhibition group.

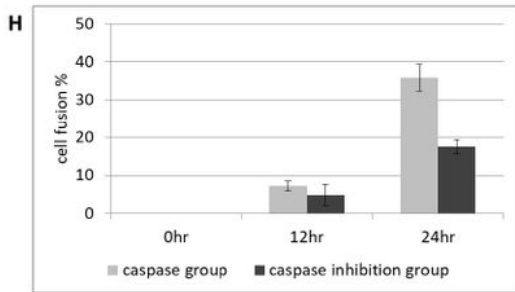
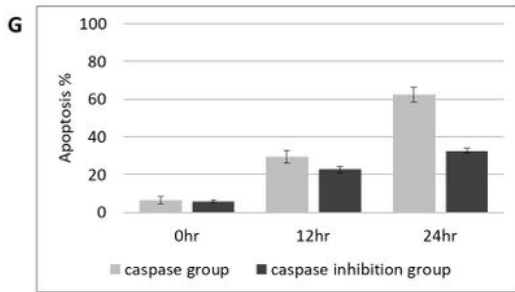
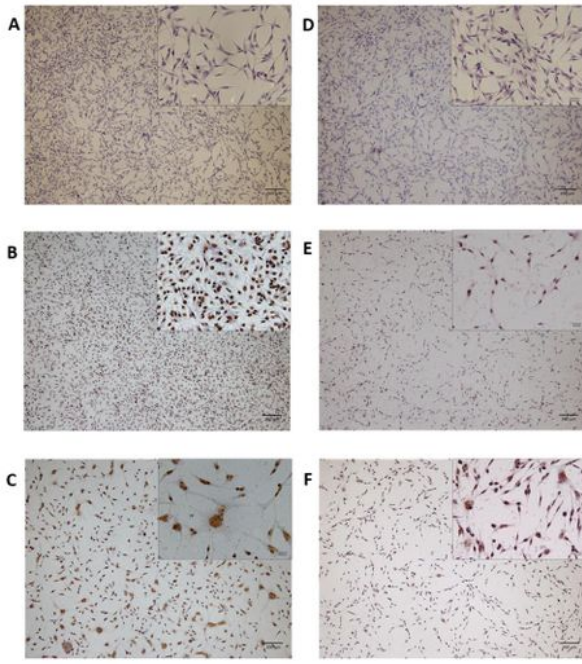


Figure 2

2a–f. Microscopic views of two groups of BHK-21 cells after NDV challenged for 0, 12, and 24 h; samples were treated with TdT-FragEL™ DNA Fragmentation Detection Kit, and cells with nuclear showing brownish color are undergoing apoptosis, while the cells with blue nuclear are living cells. 2a–2c are images of the caspase group and 2D–2F are images of the caspase inhibition group. Figure 2a–2f is magnified, scale bar = 200.0 μm (big) and scale bar = 50.0 μm (small). 2g and 2h. The trend of apoptosis

rate in two groups of BHK-21 cells under different time periods of NDV challenge, the increasing tendency of apoptosis and cell fusion with or without addition of caspase inhibitor z-VAD-fmk is confirmed by TUNEL assay. Figure 2g x-axis represents time after NDV challenge while y-axis is percentage of cells undergoing apoptosis. Results are shown in the form of mean value \pm SD for the three experiments. Figure 2h is the x-axis representing time after NDV challenge while y-axis stands for percentage of cell undergoing fusion. The results are shown in the form of mean value \pm SD for the three experiments.

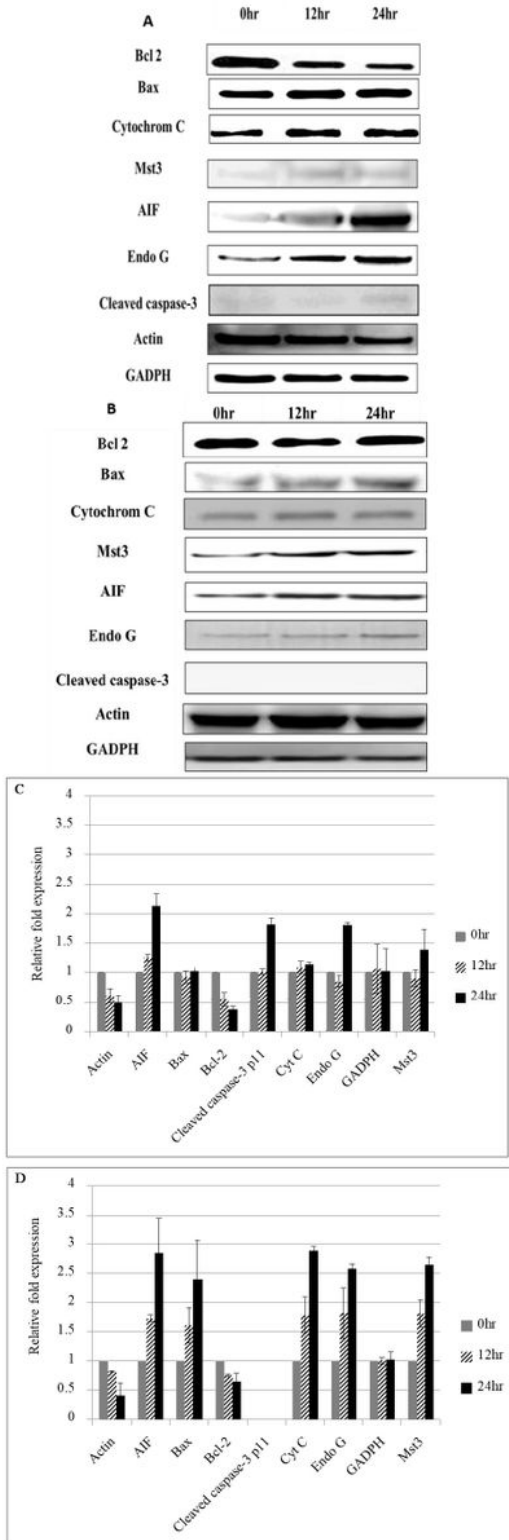


Figure 3

Influence of the expression of apoptosis-associated proteins at different times in BHK-21 cells treated with NDV and the caspase inhibitor z-VAD-fmk at the final concentration of 100 μ M. The proteins detected were the proapoptotic proteins Bax, cytochrome C, Mst3, AIF, Endo G, and cleaved caspase-3, the antiapoptotic protein Bcl-2, internal control GADPH, and actin. (3a) After BHK-21 treatment with NDV for 0, 12, and 24 h, the caspase-dependent apoptosis-associated proteins were expression. (3b) After BHK-21 treatment with NDV for 0, 12, and 24 h, the caspase-independent apoptosis-associated proteins were expression. (3c) The graph represents protein expression in the caspase-dependent group. The x-axis represents apoptosis-associated proteins and the y-axis represents the relative fold expression, challenge time as 0, 12, and 24 h. (3d) The graph represents protein expression in the caspase inhibition group. The x-axis represents apoptosis-associated proteins and the y-axis represents the relative fold expression, challenge time as 0, 12, and 24 h.

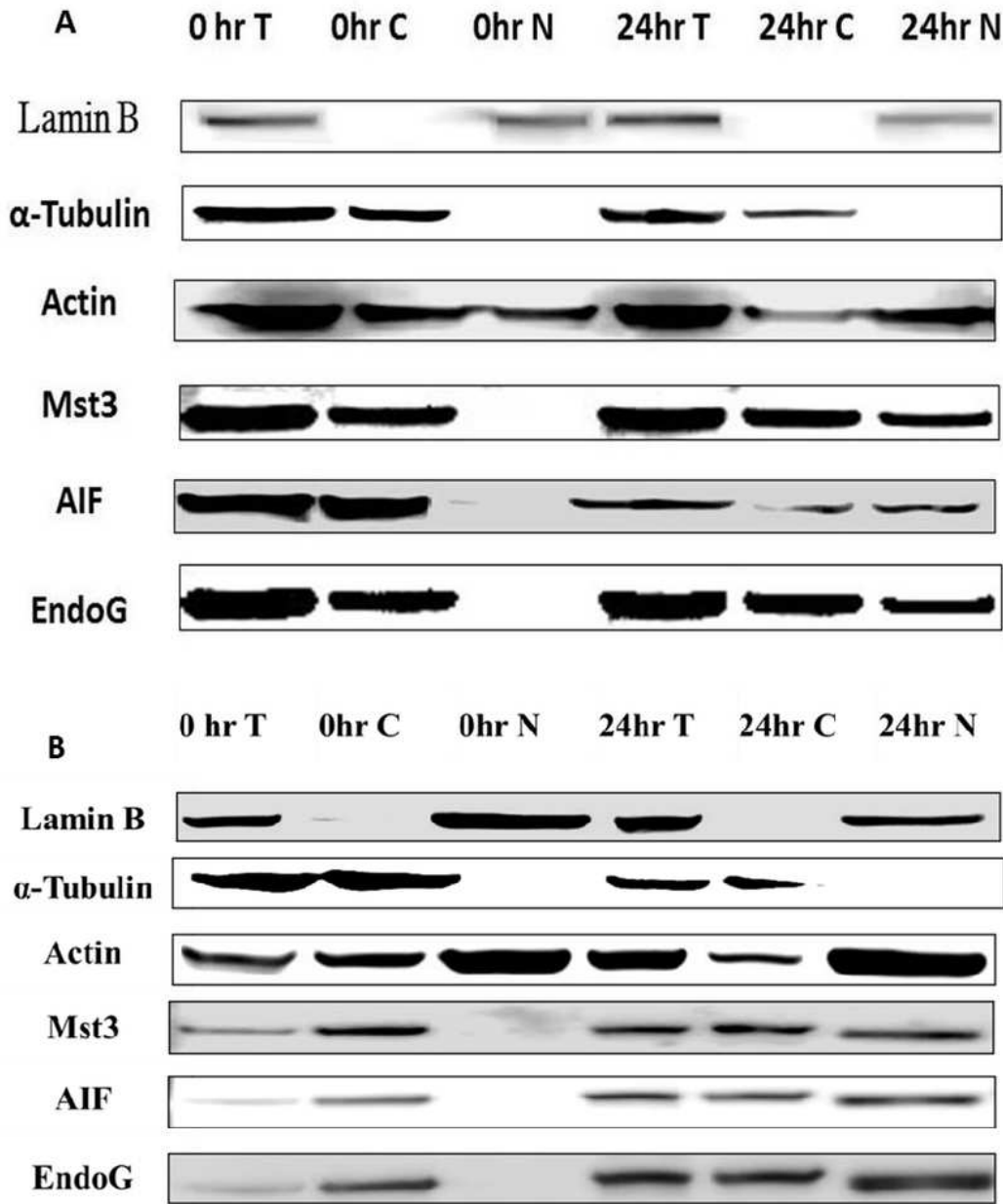


Figure 4

The cytoplasm and nucleus are shown separately to depict the changes in the positions of proteins. Lamin B is the internal control for the nuclear fraction, α -tubulin is the internal control for the cytoplasmic fraction, and actin is the internal control for the total cell. T: total protein; C: cytoplasmic protein; N: nucleus protein. (4a) NDV challenged BHK-21 cells at 0 and 24 h (caspase group). Mst3, AIF, and Endo G were transferred from the cytoplasm to the nucleus in the cells. (4b) NDV challenged BHK-21 cells at 0

and 24 h (caspase inhibition group). The Mst3, AIF, and Endo G proapoptotic proteins were similar to those in the caspase group, which help in performing apoptosis in BHK-21 cells.

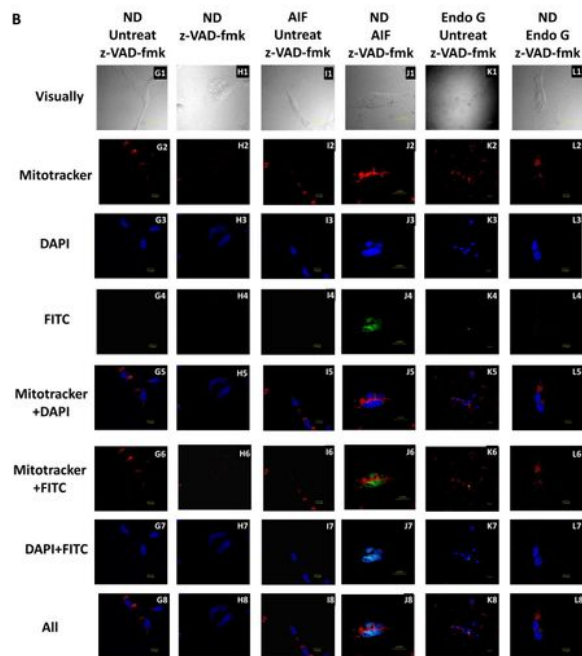
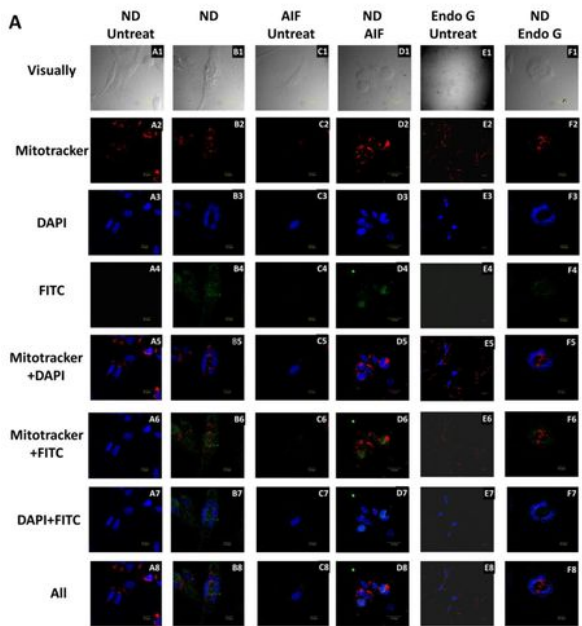


Figure 5

The Endo G and AIF were transferred from the cytoplasm to the nucleus. The green color represents NDV, Endo G, and AIF (FITC). The red color represents the mitochondria (Mitoracker). The blue color represents

the nucleus (DAPI). (5aA) The BHK-21 was treated NDV 0 and 24 h in apoptosis caspase-dependent study. (5bB) The BHK-21 was treated NDV 0 and 24 h in apoptosis caspase-independent study.